

AttentionPredictor: Temporal Pattern Matters for Efficient LLM Inference

Qingyue Yang^{1*} Jie Wang^{1†} Xing Li² Zhihai Wang¹ Chen Chen² Lei Chen² Xianzhi Yu²
Wulong Liu² Jianye Hao^{2,3} Mingxuan Yuan² Bin Li¹

¹MoE Key Laboratory of Brain-inspired Intelligent Perception and Cognition,
University of Science and Technology of China

²Noah’s Ark Lab, Huawei Technologies

³College of Intelligence and Computing, Tianjin University

Abstract

With the development of large language models (LLMs), efficient inference through Key-Value (KV) cache compression has attracted considerable attention, especially for long-context generation. To compress the KV cache, recent methods identify critical KV tokens through heuristic ranking with attention scores. However, these methods often struggle to accurately determine critical tokens as they neglect the *temporal patterns* in attention scores, resulting in a noticeable degradation in LLM performance. To address this challenge, we propose AttentionPredictor, which is the first learning-based critical token identification approach. Specifically, AttentionPredictor learns a lightweight convolution model to capture spatiotemporal patterns and predict the next-token attention score. An appealing feature of AttentionPredictor is that it accurately predicts the attention score while consuming negligible memory. Moreover, we propose a cross-token critical cache prefetching framework that hides the token estimation time overhead to accelerate the decoding stage. By retaining most of the attention information, AttentionPredictor achieves $16\times$ KV cache compression with comparable LLM performance, significantly outperforming the state-of-the-art. The code is available at <https://github.com/MIRALab-USTC/LLM-AttentionPredictor>.

1 Introduction

Large language models (LLM) like OpenAI o1 (OpenAI, 2024) have shown impressive scalability and effectiveness in tackling complex tasks through long chain-of-thought (CoT) reasoning and multi-turn conversations (Minaee et al., 2024; Huang et al., 2024). However, these long-context tasks require LLMs to handle extremely lengthy contexts, presenting computational and memory challenges for LLMs (Zhou et al., 2024). Specifically, the key-value cache (KV cache), which holds the attention keys and values during generation to prevent re-computations, consumes huge GPU memory (Li et al., 2024a). For example, for a model with 7 billion parameters, the parameters consume only 14 GB of memory whereas the KV cache requires around 72 GB with the 128K prompt length (Yang et al., 2024). As the decoding latency and memory footprint scale with the KV cache, it is important to compress the KV cache as the prompt expands.

Many attention sparsity-based methods are proposed to compress the KV cache in the sequence dimension. Previous works have shown that a small portion of tokens dominate the attention distribution, substantially determining token generation precision (Liu et al., 2023; Zhang et al.,

*This work was done when Qingyue Yang was an intern at Huawei.

†Corresponding author. Email: jiewangx@ustc.edu.cn.

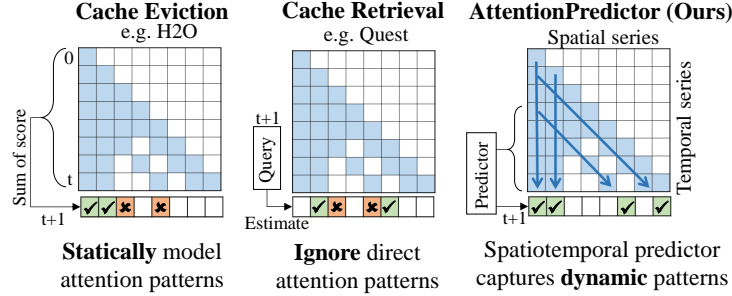


Figure 1: A comparison of H2O, Quest, and AttentionPredictor for identifying critical tokens in the next step with history attention score. Our learning-based spatiotemporal predictor captures the dynamic attention patterns and accurately predicts next-step attention scores.

2023; Ge et al., 2024). Therefore, we can dramatically reduce the cache size by computing attention sparsely with only the critical tokens, while maintaining LLM performance. Cache eviction methods (Zhang et al., 2023; Xiao et al., 2024; Li et al., 2024b) use heuristic ranking with attention scores to identify critical keys and values and evict the less relevant ones. However, heuristic scoring methods can only model static patterns and struggle to identify critical tokens accurately, causing these methods to suffer from a degradation in LLM performance. Cache retrieval methods (Tang et al., 2024; Zhang et al., 2024a) identify critical tokens by approximating attention using compressed keys and the current query. Although effective, these methods demand substantial computational resources, and model accuracy tends to degrade as the compression ratio and retrieval granularity increase. In particular, Tang et al. (2024) experiences a sharp 11% accuracy drop when the retrieving page size increases from 16 to 64. Additionally, retrieval-based methods rely on the query token in the current step, limiting their ability to overlap the estimation time overhead with actual LLM inference computation in cache prefetching systems. Thus, it is essential to accurately and rapidly identify critical tokens of the KV cache.

In our paper, we explore the importance of temporal patterns in attention scores for identifying critical KV cache. Previous research has indicated that attention scores exhibit repetitive patterns (Jiang et al., 2024; Ge et al., 2024) and are intrinsic to the LLM. These findings suggest that identifying attention patterns enables the prediction of critical tokens, making cache compression possible while preserving most information as in multi-tier cache management systems (Hashemi et al., 2018; Li et al., 2021). We further observe that attention patterns have temporal characteristics, such as re-access, sequential, and seasonal, illustrated in Figure 2. To capture the attention patterns, we introduce AttentionPredictor, a time-series prediction approach to predict attention scores for critical token identification, as shown in Figure 1. Since temporal attention patterns are dynamic and difficult to capture with existing heuristic methods, our approach is the first learning-based method to address this challenge. We frame the prediction of attention scores as a spatio-temporal forecasting problem, treating token positions as spatial patterns. We then train a convolutional model to predict next-step attention scores based on historical attention time series, enabling us to accurately identify the most critical tokens during LLM decoding. Notably, the lightweight AttentionPredictor allows for accurate predictions with negligible memory consumption. Additionally, we employ distribution error calibration by periodic computing dense attention, and we apply block-wise attention compression to further improve the efficiency of prediction. By accurately identifying critical tokens, AttentionPredictor retains most of the attention information after the KV cache compression.

To further accelerate LLM decoding, we apply AttentionPredictor to our proposed KV cache management framework, a cross-token KV cache prefetching system. Current LLM serving systems offload the KV cache to the CPU to reduce the GPU memory usage of long-context generation, but CPU-GPU transfer latency of KV cache becomes a significant bottleneck. KV cache prefetching presents a solution to hide cache loading time by asynchronously loading the required KV cache in advance. In contrast to the existing cross-layer approach (Lee et al., 2024), our cross-token method can capitalize on longer transfer times, and adapt to more sophisticated and accurate methods for identifying critical tokens. Additionally, the transfer data for each token is better organized, leading to improved I/O utilization.

We evaluated our method on several representative LLMs with varying KV cache budgets. On the widely used LongBench dataset, our approach achieves comparable accuracy with $16\times$ KV

cache compression, outperforming the state-of-the-art by 41%. With 32K context, our prefetching framework achieves a $1.4\times$ speedup of per token decoding latency. In summary, we make the following contribution:

- Based on our observation of the temporal pattern in the attention score, we propose AttentionPredictor, the first learning-based critical token identification approach.
- We propose the first cross-token prefetching framework, which effectively mitigates prediction and transfer delays in the LLM decoding stage.
- Experiments on the long-context datasets demonstrate that our approach achieves comparable accuracy of LLM with $16\times$ KV cache compression.

2 Related works

2.1 Efficient LLM Inference

Several efforts have optimized pre-trained model inference efficiency from different perspectives. Speculative decoding methods (Cai et al., 2024a; Li et al., 2024c; Sun et al., 2024; Liu et al., 2024a) use smaller draft models to accelerate the auto-regressive decoding process of LLMs. Specifically, these methods employ a draft model to efficiently predict several subsequent tokens as generation results, which are then validated in parallel using the target LLM. In contrast, our approach focuses on predicting the attention scores of the next token, serving as an estimation for KV cache compression. Other methods include model compression (Frantar et al., 2023; Lin et al., 2024) and inference systems (Kwon et al., 2023b; Sheng et al., 2023; Song et al., 2024; Contributors, 2023; Zheng et al., 2024; Ye et al., 2025).

2.2 KV Cache Compression

Many methods are dedicated to compressing the KV cache while retaining as much information of attention as possible. Many works have found that attention scores are sparse, so sparse computation can be performed on high-score positions by estimating attention scores.

Cache eviction. These methods use heuristic approaches to identify key-value pairs of high importance and evict the less relevant ones. StreamingLLM (Xiao et al., 2024) observes that the earliest tokens have high attention scores during inference, so it only retains the initial and the recent few tokens. H2O (Zhang et al., 2023) accumulates all historical attention scores as an estimation, but suffers from the accumulation error of scores from the first few tokens being too frequent. SnapKV (Li et al., 2024b) accumulates attention scores within a recent window as an estimate and performs one-time filtering during the prefill stage. MInference (Jiang et al., 2024) inductively defines three attention patterns and pre-assigns each head a fixed compression method, determining hyperparameters by attention scores within a recent window and staying static during the decoding stage. All these methods are heuristic-based and statically model attention patterns. They struggle to capture the dynamic temporal patterns within attention scores accurately.

Cache retrieval. These methods aim to retrieve the most critical tokens with approximate attention scores. Quest (Tang et al., 2024) achieves this by using the current query and paged key to approximate the attention score. However, Quest is sensitive to the page size, and the accuracy significantly drops with large page sizes and small budgets. Similarly, PQCache (Zhang et al., 2024a) applies key quantization during the prefilling stage and reuses these quantized keys in decoding to approximate attention. Since these methods require information from the current step, they cannot use asynchronous computation to cover long estimation durations. Other methods involving KV cache quantization (Liu et al., 2024b; Hooper et al., 2024; Zhang et al., 2024b) and KV cache budget allocation (Cai et al., 2024b; Yang et al., 2024; Feng et al., 2024) are orthogonal to our token scoring approach and can be combined with our AttentionPredictor.

KV cache cross-layer prefetching. These methods hide part of the cache transfer time based on offloading the cache to the CPU. However, as the sequence length increases, the transfer time is too long to be hidden. InfiniGen (Lee et al., 2024) combines cache retrieval and prefetching by approximating the attention score for the next layer to load the critical cache. However, the estimation time increases significantly as the sequence grows, and the inference time for a single

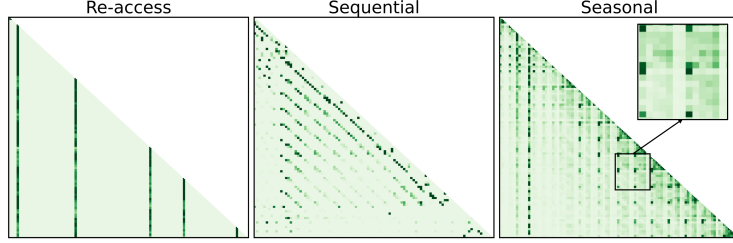


Figure 2: Visualization of three temporal attention patterns. **Re-access** shows repeated attention to specific tokens. **Sequential** shows attention progresses toward the next tokens. **Seasonal** exhibits periodic recurrence as alternating bands of high and uniform attention scores.

layer is insufficient to cover this. In contrast, our cross-token prefetching framework can hide longer estimation and transfer time within the per-token inference time.

3 Observation

3.1 Attention Temporal Patterns

Our research is motivated by the observation that attention exhibits three distinct temporal patterns: re-access, sequential, and seasonal. As shown in Figure 2, the re-access pattern occurs as vertical lines, which shows repeated attention to specific tokens. The sequential pattern is marked by diagonal lines, which show the attention moves sequentially to the next tokens. Meanwhile, the seasonal pattern is characterized by the periodic recurrence of critical tokens, which appears in Figure 2 as alternating regions of high and uniform attention scores. These patterns are consistently observed across different models and datasets.

3.2 Predict Attention by Time Series Methods

Capturing attention patterns enables accurate prediction of subsequent attention, suggesting that attention is inherently predictable. Given that LLMs are autoregressive, the process of token generation can be naturally modeled as a time series. Consequently, we propose to model attention scores as a spatiotemporal sequence, where they form a time series along the inference dimension and a spatial sequence along the token dimension. This frames attention prediction as a time series forecasting task, leveraging temporal prediction techniques to forecast the next-step attention. In contrast, existing approaches rely on static attention modeling, limiting their ability to adapt to dynamic temporal variations.

3.3 Association Between Attention Patterns and Query

To better understand why attention follows temporal patterns, we investigate the underlying causes. We find that the high continuity between queries plays a central role in shaping attention behavior. In particular, the query sequence exhibits a cosine autocorrelation of 87% at a one-step lag (in App. A), which highlights its strong similarity. High query autocorrelation, as observed in our work, is also reported in Lee et al. (2024). Based on this, we further analyze the correlation between attention in step i and step $i + 1$. Focusing on the logits before Softmax, the attention computation at step i is given as $A_i = \frac{1}{\sqrt{D}} \mathbf{Q}_i \mathbf{K}_i^\top = \frac{1}{\sqrt{D}} q_i k_{1:i}^\top$, where $q_i, k_i \in \mathbb{R}^D$ represent the query and key vectors of the token i , respectively. Assuming the query at step $i + 1$ satisfies the relationship $q_{i+1} = q_i + \Delta q$, the attention computation at step $i + 1$ can then be expressed as:

$$\begin{aligned}
 A_{i+1} &= \frac{1}{\sqrt{D}} \mathbf{Q}_{i+1} \mathbf{K}_{i+1}^\top \\
 &= \frac{1}{\sqrt{D}} q_{i+1} k_{1:i+1}^\top \\
 &= \frac{1}{\sqrt{D}} (q_i + \Delta q) k_{1:i+1}^\top \\
 &= \frac{1}{\sqrt{D}} (q_i k_{1:i+1}^\top + \Delta q k_{1:i+1}^\top)
 \end{aligned} \tag{1}$$

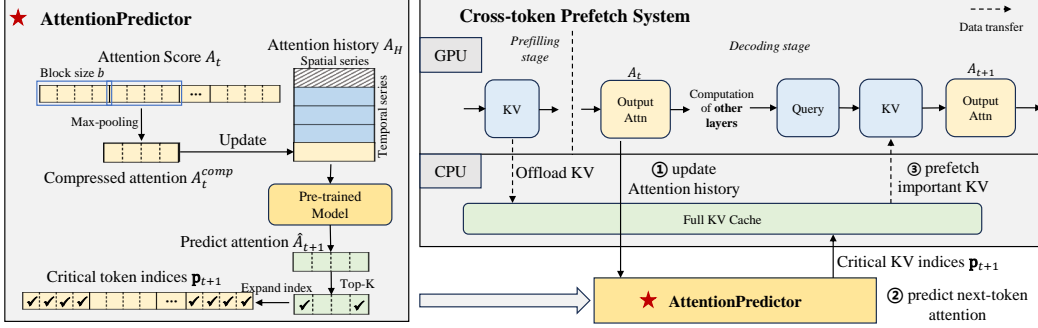


Figure 3: Overview of AttentionPredictor and cross-token prefetching framework. (a) **AttentionPredictor** formulates the attention history as a spatiotemporal sequence, and predicts the attention at the next step with a pre-trained model. To enhance efficiency, the attention history is updated in a compressed form at each decoding step. (b) **The cross-token prefetching framework** asynchronously evaluates critical tokens and fetches KV for the next token during the LLM inference, thereby accelerating the decoding stage.

Focusing on the values of A_{i+1} in the first i positions,

$$\begin{aligned} A_{i+1}[1:i] &= \frac{1}{\sqrt{D}} q_i k_{1:i}^\top + \frac{1}{\sqrt{D}} \Delta q k_{1:i}^\top \\ &= A_i + \Delta A \end{aligned} \quad (2)$$

Therefore the difference between A_i and A_{i+1} is dominated by Δq . Since q_i and q_{i+1} have high similarity, Δq is relatively small. Consequently, ΔA is small and $A_i \approx A_{i+1}$. Therefore, the critical tokens of adjacent steps are similar, which is suitable for cross-token prefetching.

4 Method

In this section, we introduce AttentionPredictor, the first learning-based method for identifying critical tokens, along with the cross-token prefetch framework for improved cache management. We begin with the problem formulation for attention prediction in Section 4.1, followed by a description of our novel AttentionPredictor in Section 4.2. Finally, Section 4.3 presents a cross-token prefetch framework that efficiently hides both evaluation and cache loading latencies.

4.1 Problem Formulation

In the language model decoding stage, we denote $\mathbf{Q}_t \in \mathbb{R}^{1 \times d}$, $\mathbf{K} \in \mathbb{R}^{t \times d}$ as the query tensor and key tensor used for generate token t , respectively. Specifically, we denote $\mathbf{K}_i \in \mathbb{R}^{1 \times d}$, where $i \in \{1, 2, \dots, t\}$, as the key tensor for token i , and $\mathbf{K} = \mathbf{K}_{1:t}$ as the complete key tensor. The attention at step t is calculated as:

$$A_t = \text{Softmax} \left(\frac{1}{\sqrt{d}} \mathbf{Q}_t \mathbf{K}^\top \right), A_t \in \mathbb{R}^{1 \times t}. \quad (3)$$

The sparsity-based KV cache compression seeks to find a subset of keys with budget B that preserves the most important attention values. Specifically, the set of selectable key positions is $\Gamma = \{\{\mathbf{p}\} = \{p_i\}_{i=1}^B \mid p_i \in \{1, 2, \dots, t\}, p_i \neq p_j, \forall i, j = 1, 2, \dots, B\}$. We define the **attention recovery rate** as:

$$R_{rec} = \frac{\sum_{i=0}^B A_{t,p_i}}{\|\mathbf{A}_t\|_1}, \quad (4)$$

which reflects the amount of information preserved after compression. A higher recovery rate R_{rec} indicates less information loss caused by KV cache compression. Therefore, the goal of KV cache compression can be formulated as finding the positions \mathbf{p} that maximize R_{rec} , i.e.,

$$\max_{\mathbf{p} \in \Gamma} R_{rec}. \quad (5)$$

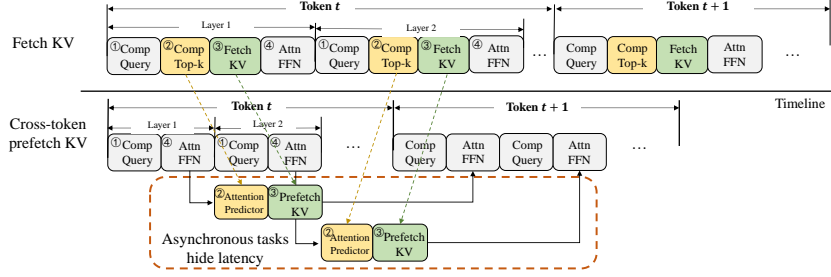


Figure 4: Timeline of our proposed cross-token prefetching. By asynchronously loading the critical KV cache for the next token, our framework hides the token evaluation and transfer latency, accelerating the decoding stage of LLM inference.

To determine the positions \mathbf{p} , existing methods typically employ heuristic approaches to score the attention at step t , represented as $S_t \in \mathbb{R}^{1 \times t}$, and then select the top B positions. For example, the well-known method H2O (Zhang et al., 2023) accumulates historical attention scores, where $S_t = \sum_{n=1}^{t-1} A_n$. In this paper, we predict the attention of step t as \hat{A}_t and use it as S_t .

After identifying the critical token positions \mathbf{p} , the attention is computed sparsely $A^{\text{sparse}} = \text{Softmax}\left(\frac{1}{\sqrt{d}} \mathbf{Q} \mathbf{K}^{\text{sparse} \top}\right)$, with selected keys $\mathbf{K}^{\text{sparse}} = \text{concate}\{\mathbf{K}_{p_i}\}$.

4.2 AttentionPredictor: A Spatiotemporal Predictor

Prediction formulation. We formulate the attention history $A_H \in \mathbb{R}^{t \times t}$ as a spatiotemporal sequence. The first dimension of A_H corresponds to the time series over the decoding steps, while the second dimension represents a sparse series over different keys. We then train a model to predict the attention for step t as $\hat{A}_{t+1} = F(A_H)$, where $F(\cdot)$ denotes the model function. For efficiency, we limit the time steps of A_H using a hyperparameter H , so that the input to the predictor is $A_H \in \mathbb{R}^{H \times t}$.

Model design. To capture spatiotemporal features, we use a convolutional neural network (CNN) composed of two 2D convolution layers followed by a 1D convolution layer. The 2D convolutions capture spatiotemporal features at multiple scales, while the 1D convolution focuses on the time dimension, extracting temporal patterns across time steps. By replacing the fully connected layer with a 1D convolution kernel, the model adapts to the increasing spatial dimension, without data segmentation or training multiple models. Compared to an auto-regressive LSTM (Graves & Graves, 2012), the CNN is more lightweight and offers faster predictions, maintaining a prediction time shorter than the single-token inference latency. Additionally, when compared to an MLP (Rumelhart et al., 1986) on time-series dimension, the CNN is more effective at capturing spatial features, which improves prediction accuracy.

Training strategy. Our model is both data-efficient and generalizable. We train the model only on a small subset of attention data, specifically approximately 3% extracted from the dataset. The model performance on the entire dataset shows our model effectively captures the patterns (see Section 5.3). Additionally, due to the temporal characteristics of attention inherent in the LLM, a single model can generalize well across various datasets. For example, our model trained on LongBench also performs well on the GSM8K dataset, highlighting the generalization capability of AttentionPredictor.

Block-wise attention compression. To speed up prediction, we apply attention compression before computation. By taking advantage of the attention’s locality, AttentionPredictor predict attention and identify critical tokens in blocks. Inspired by Tang et al. (2024), we use the maximum attention value in each block as its representative. Specifically, max-pooling is applied on A with a kernel size equal to the block size b , as $A_t^{\text{comp}} = \text{Maxpooling}(A_t, b)$, reducing prediction computation to roughly $\frac{1}{b}$.

Distribution error calibration. Due to the sparsity of attention computation, the distribution of attention history A_H used for prediction may deviate from the distribution of dense attention. This deviation tends to accumulate over decoding, particularly as the output length increases. To mitigate this issue and enhance prediction accuracy, we introduce a distribution error calibration technique to correct these deviations. Specifically, we calculate and store the full attention score every M steps, effectively balancing accuracy with computational efficiency.

Overall process. As shown in Figure 3 and Algorithm 1, AttentionPredictor prepares an attention history queue in the prefilling stage, and predicts attention during the decoding stage. First, the A_t from the LLM is compressed to A_t^{comp} using block-wise attention compression. Next, A_H is updated with A_t^{comp} . The next step attention \hat{A}_{t+1} is then predicted with the pretrained model. From \hat{A}_{t+1} , the top-K positions are selected with a budget of B/b , since \hat{A}_{t+1} is in compressed form. Finally, the indices are expanded with b to obtain the final critical token positions \mathbf{p} .

Algorithm 1 Identify Critical Tokens

Input: Attention scores A_t , Attention history A_H , Block size b , KV budget B

Output: Critical KV token positions \mathbf{p}

- 1: Pad A_t to the nearest multiple of b with zero
 - 2: $A_t^{comp} \leftarrow \text{MaxPooling}(A_t, b)$
 - 3: $A_H \leftarrow \text{Update}(A_H, A_t^{comp})$
 - 4: $\hat{A}_{t+1} \leftarrow \text{Prediction model}(A_H)$
 - 5: Positions $\leftarrow \text{Top-K}(\hat{A}_{t+1}, B/b)$
 - 6: $\mathbf{p} \leftarrow \text{Expand}(\text{Positions}, b)$
- Return** positions \mathbf{p}
-

4.3 KV Cache Cross-token Prefetching

To address the increased memory cost of longer contexts, current LLM systems offload the KV cache to the CPU, but I/O transfer latency becomes the new significant bottleneck in inference. KV cache prefetching offers a solution by asynchronously loading important cache portions in advance, hiding retrieval time. We introduce the cross-token KV cache prefetching framework, which differs from the cross-layer method in Infinigen (Lee et al., 2024) by leveraging longer transfer times and enhancing data integration. Specifically, our implementation involves a prefetching process for each layer. As illustrated in Figure 3, during the prefill phase, the computed KV cache is completely offloaded to the CPU without compression. Then, AttentionPredictor forecasts the critical token indices \mathbf{p} for the next step. The framework then prefetches the KV cache with \mathbf{p} for the next step onto the GPU. Concurrently, the GPU processes inference for other layers, so the maximum time available for prediction and cache loading corresponds to the inference time per token. Subsequently, the GPU utilizes the query for the next step along with the prefetched partial KV cache to calculate the sparse attention. The attention history is then updated with the newly computed attention scores. The timeline of cross-token prefetching can be seen in Figure 4.

5 Experimental Results

5.1 Settings

Tasks. We use the LongBench (Bai et al., 2024) dataset for long context evaluation. LongBench is a widely used benchmark for long-context LLM inference. It consists of 16 datasets covering 6 tasks, including single- and multi-document QA (SQA and MQA), summarization, few-shot learning, synthetic tasks, and code completion. LongBench uses different metrics for each dataset and calculates an average score to measure overall performance. See details in App. C.2.

We employ the GSM8K (Cobbe et al., 2021) dataset, a mathematics dataset annotated with CoT (Chain-of-Thought) reasoning processes, for evaluating CoT tasks. To evaluate the performance of our method with varying prompt lengths, we adjust the few-shot number. The evaluation metric is the accuracy of the final computational results.

Baselines. We select four sparse attention approaches as our baselines. These include three cache eviction methods, StreamingLLM (Xiao et al., 2024), H2O (Zhang et al., 2023), SnapKV (Li et al., 2024b) and one cache retrieval method Quest (Tang et al., 2024). For a fair comparison, SnapKV’s window size is set to 64, consistent with our setting. Aside from this modification, we use the official implementations and default parameters of the methods for reproducing the experiments. More details in App. C.1.

We choose two widely used long-context models for our evaluation: LongChat-v1.5-7b-32k (Kwon et al., 2023a) with 32K context length and LLaMA-3.1-8B-Instruct (Meta AI, 2024) with 128K context length.

Implementation details. *Predictor Preparation.* AttentionPredictor predictor consists of three convolutional layers, with 3×3 kernels in the first two layers and a 1×1 kernel in the last layer. For each LLM, the AttentionPredictor models are trained on a small subset of the datasets, where five samples (around 3%) were selected from each task in the LongBench dataset. During training, only decoding-stage attention was utilized. The trained AttentionPredictor models are evaluated on all tasks, including LongBench and GSM8K. The impressive results on GSM8K highlight the generalization capabilities and effectiveness of our approach.

Hyper-parameters. We set the history step H to 64, the block size b to 16 and the calibration step M to 5. Performance analysis of these hyperparameters is discussed in subsection 5.4. Follow Quest (Tang et al., 2024), we did not apply our method or any other algorithms to the first two layers of the LLM. Following the settings of H2O and StreamingLLM, We allocated the budget equally to the prefix and local tokens, assigning 64 tokens each. The remaining KV budget is allocated to intermediate tokens, determined by the prediction model. We conducted experiments on NVIDIA A800 (80GB) GPUs.

5.2 Attention Recovery Rate

We first evaluate the attention recovery rate R_{rec} of AttentionPredictor, defined as the proportion of attention scores over critical tokens identified by the method relative to the total scores as defined in Equation 4, which reflects the intermediate information loss caused by KV cache compression methods. On the three representative tasks—QA, summary, and mathematical reasoning—with different KV cache budgets, AttentionPredictor consistently achieves a higher average recovery rate compared to H2O(Zhang et al., 2023) and Quest (Tang et al., 2024) as shown in Table 1. This demonstrates that our method accurately identifies the positions of critical tokens, thereby minimizing information loss. Notably, with the KV budget of 512, AttentionPredictor shows a significant advantage over Quest, achieving a 7% higher average recovery rate, emphasizing our robustness under the extremely high ($20\times$) compression ratio. Furthermore, in the mathematical reasoning task, block-retrieval method Quest shows substantial recovery loss, suggesting potential limitations in this complex task. In contrast, our block-prediction method alleviates this issue, further underscoring its reliability.

Table 1: The attention recovery rate (%) across different cache sizes (higher is better).

| Llama-3.1-8B | | | | | |
|--------------|--------------------|--------------|--------------|--------------|--------------|
| KV Budget | Method | QA | Summary | Math | Average |
| 512 | H2O | 79.97 | 79.36 | 88.23 | 82.52 |
| | Quest | 80.85 | 72.37 | 78.14 | 77.12 |
| | AttentionPredictor | 84.79 | 79.73 | 87.77 | 84.10 |
| 1024 | H2O | 85.70 | 83.49 | 91.37 | 86.85 |
| | Quest | 87.69 | 81.02 | 85.52 | 84.74 |
| | AttentionPredictor | 90.63 | 85.16 | 92.04 | 89.28 |
| 2048 | H2O | 91.58 | 88.37 | 94.79 | 91.58 |
| | Quest | 93.40 | 88.12 | 92.04 | 91.19 |
| | AttentionPredictor | 95.03 | 90.30 | 95.52 | 93.62 |
| 4096 | H2O | 96.59 | 93.49 | 97.97 | 96.02 |
| | Quest | 97.37 | 93.93 | 97.06 | 96.12 |
| | AttentionPredictor | 98.07 | 94.88 | 98.26 | 97.07 |

5.3 Final Accuracy Evaluation

Results on LongBench. We evaluate our method on various long-context tasks in the LongBench benchmark, with the KV cache budgets ranging from 512 to 4096. We restrict H2O’s attention to the past 64 steps to ensure fairness and denote this variant as H2O+. As shown in Table 2, AttentionPredictor surpasses the performance of all SOTA KV cache eviction and retrieval methods across various KV budgets and LLMs. Notably, the average performance loss compared to the full cache is less than 0.5% across all cache budgets. This demonstrates the ability of our method to effectively model attention patterns and precisely predict the locations of critical tokens. Furthermore, under an extremely sparse budget setting of 4% (512/13K), our approach results in only a 0.44% decrease in performance compared to the full cache, indicating a 76% improvement over the state-of-the-art Quest method, which suffers a 1.84% reduction.

Results on CoT reasoning. As shown in Table 3, we evaluate our method on the mathematical reasoning dataset GSM8K with LLaMA-3.1. By adjusting the number of few-shot examples to simulate the long-context reasoning process with short and long CoTs, we generate input lengths

Table 2: The evaluation results from the LongBench dataset across 512, 1024, 2048, and 4096 KV cache budgets.

| Budget | Method | SQA | MQA | Summary | Few-shot | Synthetic | Code | Average \uparrow | SQA | MQA | Summary | Few-shot | Synthetic | Code | Average \uparrow |
|-------------|--------------------|----------------------|--------------|--------------|--------------|--------------|--------------|--------------------|-----------------------|--------------|--------------|--------------|--------------|--------------|--------------------|
| | | Longchat-v1.5-7b-32k | | | | | | | LLaMA-3.1-8B-Instruct | | | | | | |
| Full | Full cache | 31.07 | 23.95 | 24.70 | 63.80 | 15.25 | 54.86 | 36.06 | 43.59 | 46.00 | 26.14 | 68.78 | 52.29 | 52.51 | 48.17 |
| 512 | StreamingLLM | 19.96 | 19.20 | 20.68 | 57.71 | 2.75 | 49.73 | 28.65 | 28.69 | 39.77 | 21.81 | 59.44 | 53.25 | 50.41 | 41.17 |
| | H2O+ | 25.36 | 21.77 | 21.83 | 57.85 | 13.75 | 52.99 | 32.07 | 33.68 | 41.86 | 23.42 | 59.60 | 53.83 | 51.97 | 43.02 |
| | SnapKV | 27.37 | 23.44 | 21.87 | 60.54 | 12.75 | 55.91 | 33.36 | 39.46 | 42.61 | 23.69 | 65.58 | 51.70 | 51.15 | 45.02 |
| | Quest | 28.75 | 20.57 | 24.13 | 60.57 | 20.75 | 51.09 | 34.34 | 41.27 | 43.63 | 25.65 | 65.99 | 55.33 | 46.84 | 46.33 |
| | AttentionPredictor | 29.27 | 23.99 | 23.67 | 63.07 | 13.25 | 55.16 | 35.10 | 43.44 | 45.75 | 25.68 | 66.42 | 56.50 | 50.99 | 47.73 |
| 1024 | StreamingLLM | 22.89 | 19.84 | 21.94 | 60.65 | 3.75 | 53.23 | 30.84 | 31.73 | 37.51 | 21.98 | 64.69 | 51.25 | 51.26 | 42.35 |
| | H2O+ | 26.98 | 22.38 | 22.92 | 61.10 | 14.00 | 54.67 | 33.58 | 37.00 | 42.28 | 24.32 | 60.81 | 54.28 | 52.21 | 44.25 |
| | SnapKV | 28.46 | 23.85 | 22.98 | 62.75 | 14.00 | 55.84 | 34.63 | 40.62 | 43.30 | 24.78 | 67.14 | 53.81 | 52.57 | 46.37 |
| | Quest | 30.31 | 21.41 | 24.60 | 63.40 | 17.50 | 52.47 | 35.29 | 42.00 | 43.87 | 26.03 | 66.89 | 54.53 | 48.87 | 46.92 |
| | AttentionPredictor | 30.18 | 24.28 | 24.20 | 63.81 | 14.00 | 54.38 | 35.62 | 43.61 | 45.02 | 25.65 | 68.22 | 53.00 | 52.20 | 47.80 |
| 2048 | StreamingLLM | 24.79 | 20.44 | 23.62 | 61.52 | 5.75 | 52.62 | 31.99 | 34.39 | 36.61 | 24.63 | 64.80 | 45.13 | 44.99 | 41.64 |
| | H2O+ | 27.51 | 22.91 | 21.51 | 62.58 | 14.50 | 54.66 | 34.09 | 40.55 | 43.78 | 24.94 | 65.51 | 53.36 | 53.58 | 46.34 |
| | SnapKV | 29.77 | 24.27 | 23.71 | 63.53 | 14.25 | 56.69 | 35.50 | 42.77 | 44.79 | 25.31 | 67.19 | 53.32 | 54.35 | 47.44 |
| | Quest | 31.64 | 23.90 | 24.51 | 64.43 | 15.75 | 53.13 | 36.14 | 43.73 | 44.75 | 25.91 | 69.39 | 54.25 | 50.01 | 48.00 |
| | AttentionPredictor | 30.91 | 24.37 | 24.34 | 64.60 | 15.25 | 54.52 | 36.15 | 42.78 | 45.25 | 26.09 | 68.26 | 55.38 | 51.81 | 48.04 |
| 4096 | StreamingLLM | 29.63 | 20.01 | 23.64 | 56.18 | 7.75 | 55.36 | 32.36 | 41.63 | 38.82 | 24.44 | 58.95 | 41.15 | 52.27 | 42.63 |
| | H2O+ | 30.07 | 23.72 | 21.74 | 63.16 | 14.75 | 54.66 | 35.06 | 43.14 | 45.21 | 25.52 | 66.14 | 53.29 | 53.61 | 47.45 |
| | SnapKV | 30.52 | 24.35 | 24.54 | 63.80 | 14.50 | 56.70 | 35.99 | 42.87 | 45.34 | 25.79 | 67.63 | 54.09 | 53.39 | 47.84 |
| | Quest | 30.94 | 22.98 | 24.61 | 64.19 | 15.50 | 53.62 | 35.83 | 43.46 | 44.51 | 25.77 | 68.23 | 53.21 | 50.16 | 47.59 |
| | AttentionPredictor | 30.78 | 24.50 | 24.65 | 64.19 | 14.75 | 54.85 | 36.10 | 43.14 | 45.45 | 25.94 | 68.07 | 54.41 | 51.21 | 47.92 |

of 4K, 8K, and 16K. Unlike long-context tasks, CoT mathematical reasoning tasks present distinct challenges. For example, the retrieval-based SOTA method, Quest, excels on long-context benchmarks but performs poorly on CoT tasks, showing a 16.91% accuracy drop at a sequence length of 16K. In contrast, AttentionPredictor achieves a significantly smaller accuracy loss of just 2.05%. Moreover, across all sequence lengths, our method outperforms baselines in most cases. Under a 25% cache budget, it even exceeds the accuracy of the full cache, achieving lossless performance. H2O+ also performs well in this task, likely due to half of the cache budget being on local tokens, which remain unaffected by variations of the few-shot. Additionally, H2O+ includes only 64 steps of historical information, limiting the influence of irrelevant attention scores.

5.4 Ablation Study

The effects of varying hyperparameters on the performance of AttentionPredictor with Longchat are studied. Three key hyperparameters, including history step, calibration step, and block size, are evaluated across six tasks from the LongBench dataset. Detailed task-specific results are available in App. C.5. Additionally, the prediction model implementation is also evaluated.

Block size b . As shown in Figure 5a, AttentionPredictor maintains superior average performance across block sizes from 8 to 64. While performance degradation occurs with increasing block size due to coarser token positioning, our method exhibits a milder decline compared to Quest’s block-granularity KV cache retrieval. The performance drop in Quest may be attributed to the loss of total attention score information when the min-max based attention score upper bound estimation of each block is used for retrieved, leading to inaccuracies in block identification. In contrast, our approach accurately captures attention patterns, thereby improving critical block identification and mitigating the drawbacks of block-wise retrieval.

Calibration step M . Figure 5b shows the average performance of AttentionPredictor with calibration steps ranging from 1 to 20. Performance improves with shorter calibration intervals, indicating that the calibration scheme reduces cumulative errors caused by differences between sparse and original attention distributions. However, higher calibration frequencies increase computational costs, creating a trade-off between accuracy and efficiency.

History step H . As depicted in Figure 5c, we evaluate the average accuracy of AttentionPredictor over a range of history steps. Overall, the performance gap compared to the full cache remains

Table 3: Evaluation results on the CoT dataset.

| GSM8K+LLaMA-3.1 | | | | | |
|---------------------------|--------|---------------|--------------|--------------|--------------|
| Method | Budget | Prompt length | | | Average |
| | | 4K | 8K | 16K | |
| Full cache | Full | 56.79 | 55.27 | 54.13 | 55.40 |
| StreamingLLM | 1K | 54.74 | 49.96 | 50.94 | 51.88 |
| H2O+ | 1K | 57.16 | 52.01 | 52.16 | 53.78 |
| Quest | 1K | 48.52 | 45.26 | 37.22 | 43.67 |
| SnapKV | 1K | 53.45 | 48.67 | 49.20 | 50.44 |
| AttentionPredictor | 1K | 57.16 | 53.75 | 52.08 | 54.33 |

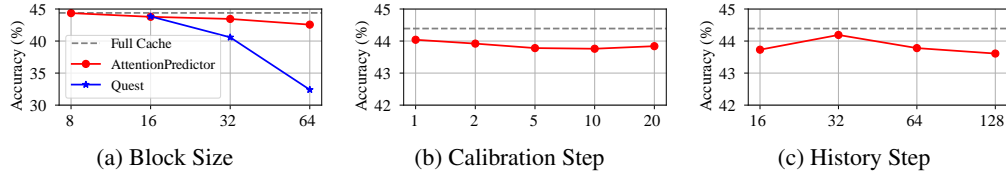


Figure 5: Hyper-parameter ablation on Longchat with LongBench.

consistently small. Notably, the middle value of H maximizes performance by providing the necessary information for pattern recognition, while mitigating redundancy caused by the decaying self-correlation of attention scores.

Prediction model. We evaluate the performance of various prediction model implementations. MLP is applied to the sequence dimension to handle variations in attention length. For LSTM, attention is divided into 16 width blocks and predictions are independent for each block, referred to as LSTM-block in Table 4. Similarly, CNN-block utilizes a block-wise prediction approach, employing a fully connected layer for fixed block lengths. Finally, the CNN model, as the primary setting in our experiments, predicts all attention scores simultaneously. As reported in Table 4, CNN outperforms other models, achieving the highest attention recovery rate by effectively capturing attention patterns. MLP failed to account for neighboring token interactions, while LSTM-block and CNN-block were restricted to block-level information without global context. Notably, CNN also required the fewest parameters and was the most memory-efficient during inference.

5.5 Efficiency

We evaluate the final LLM inference acceleration of our method in Table 5, using the widely adopted cross-layer prefetching system with cache offloading as the baseline, which is implemented in Wolf et al. (2020). By reducing cache transfers, AttentionPredictor achieves a $1.2\times$ speedup in per-token decoding with a 1K budget, demonstrating more efficient inference. The added token evaluation time is negligible, leading to a substantial overall speed improvement. Furthermore, we apply AttentionPredictor to our proposed cross-token prefetching framework, which enables asynchronous cache retrieval and I/O transferring between layers. This integration yields an additional $1.4\times$ speedup in the decoding stage, further highlighting the effectiveness of our approach.

Table 4: Attention recovery rate and parameter numbers of different model implementation.

| LongBench+Longchat | | |
|--------------------|--------------|---------------|
| Model type | Total params | Recovery rate |
| MLP | 49K | 92.88 |
| LSTM-block | 3.2M | 91.75 |
| CNN-block | 21K | 91.94 |
| CNN | 4.9K | 93.65 |

Table 5: The decode latency of per token of LLaMA-3.1-8B with 32K context length.

| Method | Decode latency(s) | Speed |
|--|-------------------|-------------------------------|
| cross-layer pref. | 0.364 | 1 \times |
| cross-layer pref.+ AttentionPredictor | 0.295 | 1.2 \times |
| cross-token pref.+AttentionPredictor | 0.262 | 1.4\times |

6 Conclusion

We present AttentionPredictor, the first learning-based critical token identification approach for KV cache compression. With a lightweight convolution model, AttentionPredictor captures spatiotemporal patterns of attention score and predicts the next-token attention score accurately. Additionally, we propose the first cross-token prefetching framework, which effectively mitigates prediction and transfer delays in the LLM decoding stage. Experiments on the long-context datasets demonstrate that AttentionPredictor achieves comparable accuracy of LLM with $16\times$ KV cache compression.

References

- Bai, Y., Lv, X., Zhang, J., Lyu, H., Tang, J., Huang, Z., Du, Z., Liu, X., Zeng, A., Hou, L., Dong, Y., Tang, J., and Li, J. LongBench: A bilingual, multitask benchmark for long context understanding. In *Proceedings of the 62nd Annual Meeting of the Association for Computational Linguistics (Volume 1: Long Papers)*, pp. 3119–3137, Bangkok, Thailand, August 2024. Association for Computational Linguistics. doi: 10.18653/v1/2024.acl-long.172. URL <https://aclanthology.org/2024.acl-long.172>.
- Cai, T., Li, Y., Geng, Z., Peng, H., Lee, J. D., Chen, D., and Dao, T. Medusa: Simple LLM inference acceleration framework with multiple decoding heads. In *Forty-first International Conference on Machine Learning, ICML 2024, Vienna, Austria, July 21-27, 2024*, 2024a.
- Cai, Z., Zhang, Y., Gao, B., Liu, Y., Liu, T., Lu, K., Xiong, W., Dong, Y., Chang, B., Hu, J., et al. Pyramidkv: Dynamic kv cache compression based on pyramidal information funneling. *arXiv preprint arXiv:2406.02069*, 2024b.
- Cobbe, K., Kosaraju, V., Bavarian, M., Chen, M., Jun, H., Kaiser, L., Plappert, M., Tworek, J., Hilton, J., Nakano, R., Hesse, C., and Schulman, J. Training verifiers to solve math word problems. *arXiv preprint arXiv:2110.14168*, 2021.
- Contributors, L. Lmdeploy: A toolkit for compressing, deploying, and serving llm. <https://github.com/InternLM/lmdeploy>, 2023.
- Dao, T. Flashattention-2: Faster attention with better parallelism and work partitioning. In *The Twelfth International Conference on Learning Representations*, 2024.
- Feng, Y., Lv, J., Cao, Y., Xie, X., and Zhou, S. K. Ada-kv: Optimizing kv cache eviction by adaptive budget allocation for efficient llm inference. *arXiv preprint arXiv:2407.11550*, 2024.
- Frantar, E., Ashkboos, S., Hoefler, T., and Alistarh, D. Gptq: Accurate post-training quantization for generative pre-trained transformers. In *The Eleventh International Conference on Learning Representations*, 2023.
- Ge, S., Zhang, Y., Liu, L., Zhang, M., Han, J., and Gao, J. Model tells you what to discard: Adaptive KV cache compression for llms. In *The Twelfth International Conference on Learning Representations, ICLR 2024, Vienna, Austria, May 7-11, 2024*, 2024.
- Graves, A. and Graves, A. Long short-term memory. *Supervised sequence labelling with recurrent neural networks*, pp. 37–45, 2012.
- Hashemi, M., Swersky, K., Smith, J., Ayers, G., Litz, H., Chang, J., Kozyrakis, C., and Ranganathan, P. Learning memory access patterns. In *International Conference on Machine Learning*, pp. 1919–1928. PMLR, 2018.
- Hooper, C., Kim, S., Mohammadzadeh, H., Mahoney, M. W., Shao, Y. S., Keutzer, K., and Gholami, A. Kvquant: Towards 10 million context length llm inference with kv cache quantization. *arXiv preprint arXiv:2401.18079*, 2024.
- Huang, X., Liu, W., Chen, X., Wang, X., Wang, H., Lian, D., Wang, Y., Tang, R., and Chen, E. Understanding the planning of llm agents: A survey. *arXiv preprint arXiv:2402.02716*, 2024.
- Jiang, H., Li, Y., Zhang, C., Wu, Q., Luo, X., Ahn, S., Han, Z., Abdi, A. H., Li, D., Lin, C.-Y., et al. Minference 1.0: Accelerating pre-filling for long-context llms via dynamic sparse attention. *arXiv preprint arXiv:2407.02490*, 2024.
- Kwon, W., Li, Z., Zhuang, S., Sheng, Y., Zheng, L., Yu, C. H., Gonzalez, J., Zhang, H., and Stoica, I. Efficient memory management for large language model serving with pagedattention. In Flinn, J., Seltzer, M. I., Druschel, P., Kaufmann, A., and Mace, J. (eds.), *Proceedings of the 29th Symposium on Operating Systems Principles, SOSP 2023, Koblenz, Germany, October 23-26, 2023*, pp. 611–626. ACM, 2023a. doi: 10.1145/3600006.3613165. URL <https://doi.org/10.1145/3600006.3613165>.

- Kwon, W., Li, Z., Zhuang, S., Sheng, Y., Zheng, L., Yu, C. H., Gonzalez, J., Zhang, H., and Stoica, I. Efficient memory management for large language model serving with pagedattention. In *Proceedings of the 29th Symposium on Operating Systems Principles*, pp. 611–626, 2023b.
- Lee, W., Lee, J., Seo, J., and Sim, J. {InfiniGen}: Efficient generative inference of large language models with dynamic {KV} cache management. In *18th USENIX Symposium on Operating Systems Design and Implementation (OSDI 24)*, pp. 155–172, 2024.
- Li, H., Li, Y., Tian, A., Tang, T., Xu, Z., Chen, X., Hu, N., Dong, W., Li, Q., and Chen, L. A survey on large language model acceleration based on kv cache management. *arXiv preprint arXiv:2412.19442*, 2024a.
- Li, X., Shi, Q., Hu, G., Chen, L., Mao, H., Yang, Y., Yuan, M., Zeng, J., and Cheng, Z. Block access pattern discovery via compressed full tensor transformer. In *Proceedings of the 30th ACM International Conference on Information & Knowledge Management*, pp. 957–966, 2021.
- Li, Y., Huang, Y., Yang, B., Venkitesh, B., Locatelli, A., Ye, H., Cai, T., Lewis, P., and Chen, D. Snapkv: Llm knows what you are looking for before generation. *arXiv preprint arXiv:2404.14469*, 2024b.
- Li, Y., Wei, F., Zhang, C., and Zhang, H. EAGLE: speculative sampling requires rethinking feature uncertainty. In *Forty-first International Conference on Machine Learning, ICML 2024, Vienna, Austria, July 21-27, 2024*, 2024c.
- Lin, J., Tang, J., Tang, H., Yang, S., Chen, W.-M., Wang, W.-C., Xiao, G., Dang, X., Gan, C., and Han, S. Awq: Activation-aware weight quantization for on-device llm compression and acceleration. *Proceedings of Machine Learning and Systems*, 6:87–100, 2024.
- Liu, A., Feng, B., Xue, B., Wang, B., Wu, B., Lu, C., Zhao, C., Deng, C., Zhang, C., Ruan, C., et al. Deepseek-v3 technical report. *arXiv preprint arXiv:2412.19437*, 2024a.
- Liu, Z., Wang, J., Dao, T., Zhou, T., Yuan, B., Song, Z., Shrivastava, A., Zhang, C., Tian, Y., Re, C., et al. Deja vu: Contextual sparsity for efficient llms at inference time. In *International Conference on Machine Learning*, pp. 22137–22176. PMLR, 2023.
- Liu, Z., Yuan, J., Jin, H., Zhong, S., Xu, Z., Braverman, V., Chen, B., and Hu, X. KIVI: A tuning-free asymmetric 2bit quantization for KV cache. In *Forty-first International Conference on Machine Learning, ICML 2024, Vienna, Austria, July 21-27, 2024*, 2024b.
- Meta AI. Introducing Llama 3.1. <https://ai.meta.com/blog/meta-llama-3-1/>, 2024. [Accessed 09-01-2025].
- Minaee, S., Mikolov, T., Nikzad, N., Chenaghlu, M., Socher, R., Amatriain, X., and Gao, J. Large language models: A survey. *arXiv preprint arXiv:2402.06196*, 2024.
- OpenAI. Learning to reason with LLMs. <https://openai.com/index/learning-to-reason-with-llms/>, 2024. [Accessed 30-01-2025].
- Rumelhart, D. E., Hinton, G. E., and Williams, R. J. Learning representations by back-propagating errors. *nature*, 323(6088):533–536, 1986.
- Sheng, Y., Zheng, L., Yuan, B., Li, Z., Ryabinin, M., Chen, B., Liang, P., Ré, C., Stoica, I., and Zhang, C. Flexgen: High-throughput generative inference of large language models with a single gpu. In *International Conference on Machine Learning*, pp. 31094–31116. PMLR, 2023.
- Song, M., Tang, X., Hou, F., Li, J., Wei, W., Ma, Y., Xiao, R., Si, H., Jiang, D., Yin, S., et al. Tackling the dynamicity in a production llm serving system with sota optimizations via hybrid prefill/decode/verify scheduling on efficient meta-kernels. *arXiv preprint arXiv:2412.18106*, 2024.
- Sun, H., Chen, Z., Yang, X., Tian, Y., and Chen, B. Triforce: Lossless acceleration of long sequence generation with hierarchical speculative decoding. *arXiv preprint arXiv:2404.11912*, 2024.

- Tang, J., Zhao, Y., Zhu, K., Xiao, G., Kasikci, B., and Han, S. QUEST: query-aware sparsity for efficient long-context LLM inference. In *Forty-first International Conference on Machine Learning, ICML 2024, Vienna, Austria, July 21-27, 2024*, 2024. URL <https://openreview.net/forum?id=KzACYwOMTV>.
- Wolf, T., Debut, L., Sanh, V., Chaumond, J., Delangue, C., Moi, A., Cistac, P., Rault, T., Louf, R., Funtowicz, M., Davison, J., Shleifer, S., von Platen, P., Ma, C., Jernite, Y., Plu, J., Xu, C., Scao, T. L., Gugger, S., Drame, M., Lhoest, Q., and Rush, A. M. Transformers: State-of-the-art natural language processing. In *Proceedings of the 2020 Conference on Empirical Methods in Natural Language Processing: System Demonstrations*, pp. 38–45, Online, October 2020. Association for Computational Linguistics. URL <https://www.aclweb.org/anthology/2020.emnlp-demos.6>.
- Xiao, G., Tian, Y., Chen, B., Han, S., and Lewis, M. Efficient streaming language models with attention sinks. In *The Twelfth International Conference on Learning Representations, ICLR 2024, Vienna, Austria, May 7-11, 2024*. OpenReview.net, 2024. URL <https://openreview.net/forum?id=NG7sS51zVF>.
- Yang, D., Han, X., Gao, Y., Hu, Y., Zhang, S., and Zhao, H. Pyramidinfer: Pyramid KV cache compression for high-throughput LLM inference. In *Findings of the Association for Computational Linguistics, ACL 2024, Bangkok, Thailand and virtual meeting, August 11-16, 2024*, pp. 3258–3270, 2024.
- Ye, Z., Chen, L., Lai, R., Lin, W., Zhang, Y., Wang, S., Chen, T., Kasikci, B., Grover, V., Krishnamurthy, A., et al. Flashinfer: Efficient and customizable attention engine for llm inference serving. *arXiv preprint arXiv:2501.01005*, 2025.
- Zhang, H., Ji, X., Chen, Y., Fu, F., Miao, X., Nie, X., Chen, W., and Cui, B. Pqcache: Product quantization-based kvcache for long context llm inference. *arXiv preprint arXiv:2407.12820*, 2024a.
- Zhang, Z., Sheng, Y., Zhou, T., Chen, T., Zheng, L., Cai, R., Song, Z., Tian, Y., Ré, C., Barrett, C. W., Wang, Z., and Chen, B. H2O: heavy-hitter oracle for efficient generative inference of large language models. In Oh, A., Naumann, T., Globerson, A., Saenko, K., Hardt, M., and Levine, S. (eds.), *Advances in Neural Information Processing Systems 36: Annual Conference on Neural Information Processing Systems 2023, NeurIPS 2023, New Orleans, LA, USA, December 10 - 16, 2023*, 2023.
- Zhang, Z., Liu, S., Chen, R., Kailkhura, B., Chen, B., and Wang, A. Q-hitter: A better token oracle for efficient llm inference via sparse-quantized kv cache. *Proceedings of Machine Learning and Systems*, 6:381–394, 2024b.
- Zheng, L., Yin, L., Xie, Z., Sun, C., Huang, J., Yu, C. H., Cao, S., Kozyrakis, C., Stoica, I., Gonzalez, J. E., et al. Sglang: Efficient execution of structured language model programs. *arXiv preprint arXiv:2312.07104*, 2024.
- Zhou, Z., Ning, X., Hong, K., Fu, T., Xu, J., Li, S., Lou, Y., Wang, L., Yuan, Z., Li, X., et al. A survey on efficient inference for large language models. *arXiv preprint arXiv:2404.14294*, 2024.

A Query Similarity

We evaluate the similarity of consecutive queries. Specifically, we extract query data from LLaMA-3.1-8B using LongBench and compute the cosine autocorrelation of adjacent queries with a lag of 1. As shown in Figure 6, the heatmap illustrates the query similarity across each layer and head of the LLM. The average similarity is 86% for Longchat and 87% for LLaMA-3.1, indicating strong continuity. Furthermore, the similarity in LLaMA is more consistent across layers, while Longchat shows higher similarity in the shallower layers.

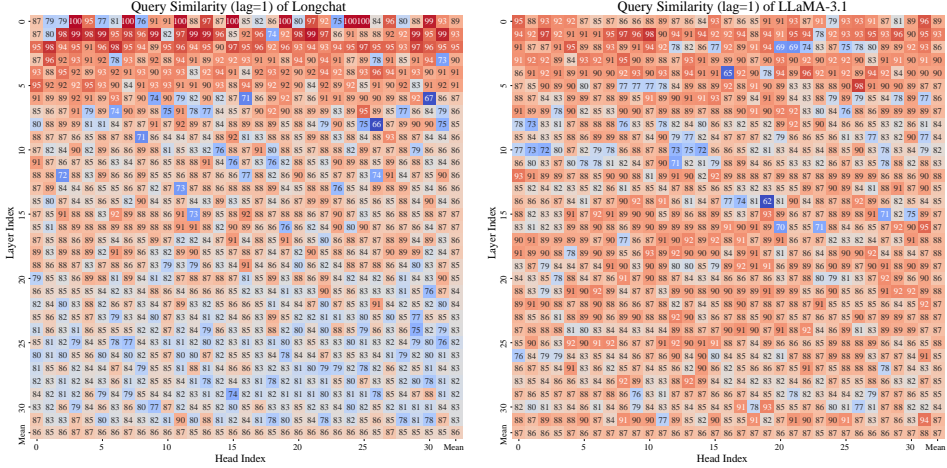


Figure 6: Query similarity of Longchat and LLaMA-3.1.

B Implementation of AttentionPredictor

Training Details. We capture the attention scores during full-cache inference as raw data. We package the attention scores of H steps, together with the $(H + 1)$ -th step’s score, as input-output pairs. The training data is block-compressed to align with the usage during LLM model inference. Specifically, the input history attention is $A_H \in \mathbb{R}^{H \times \frac{L}{b}}$ and the output attention score is $S \in \mathbb{R}^{1 \times \frac{L}{b}}$. Attention scores with insufficient lengths are padded with zeros at the end to ensure that all data within a package have the same length. For the attention at step $t + 1$, we only predict the first t positions because the last position is derived from the newly generated key, which does not need to be compressed or transferred. Notably, only the attention scores from the decoding phase are used as output data. As a result, the training dataset includes the final H steps of the pre-filling attention and all attention scores from the decoding stage. To train the model, we calculate the discrepancy between the predicted and real attention scores using mean squared error (MSE) loss. The training epoch is set to 30, and we select the model with the best attention recovery rate as shown in Equation 4.

Cross-token Prefetching. We leverage GPU parallel streams and CPU multi-threading to parallelize the token retrieval and cache transfer across different layers. Consistent with the main experiment, we maintain uncompressed caches for the first two layers to ensure higher inference accuracy.

C Experiments

C.1 Implementation of Baselines

Our experiments are based on LLMs using 16-bit floating points, and we utilize FlashAttention2 (Dao, 2024) during the prefilling stage to reduce GPU memory consumption. Since FlashAttention2 does not output intermediate attention scores, for methods that rely on historical attention, we additionally compute partial prefill attention to obtain the scores. Our batch size is fixed at 1. For all baselines, we use the official code implementations to ensure the effectiveness of the methods. Additionally, for all methods, we skip compress the first two layers of the LLM.

- StreamingLLM (Xiao et al., 2024) finds that the sink token is very important, so it retains the initial and the most recent few tokens. For StreamingLLM, we evenly distribute the budget between sink tokens and local tokens.
- H2O (Zhang et al., 2023) accumulates all historical attention scores as an estimation. We evenly distribute the budget between the heavy budget and the recent budget. Since computing the full historical data can cause OOM with longer inputs, we use the last 64 steps of historical information to calculate the heavy hitters, and denote this as H2O+. Note that accumulating all prefill attention scores causes H2O to focus on initial tokens, so this is an improvement to the method’s effectiveness.
- SnapKV (Li et al., 2024b) accumulates attention scores within a recent window as an estimate and performs one-time filtering during the prefill stage. We set the time window to a size of 64 to align with our method. Since SnapKV only performs cache compression once during the prefill stage, the number of KV tokens it uses continues to grow during decoding, resulting in a relatively lower compression ratio compared to other methods.
- Quest (Tang et al., 2024) uses the current query and paged key to approximate the attention score. We use a chunk size of 16, corresponding to the block size in our method, which is also the parameter value used in the original paper.

C.2 Details of LongBench Dataset

LongBench (Bai et al., 2024) is a carefully crafted benchmark suite designed to evaluate the capabilities of language models in processing extended documents and complex information sequences. It was developed for multi-task assessment of long-context inputs. The details of the metrics, number of words, language, and data used in LongBench are presented in Table 6.

Table 6: An overview of the dataset statistics in LongBench. ‘Source’ denotes the origin of the context. ‘Avg len’ refers to the average number of words, which is shorter than the token length after tokenization. ‘Accuracy (CLS)’ refers to classification accuracy, while ‘Accuracy (EM)’ refers to exact match accuracy.

| Dataset | Source | Avg len | Metric | Language | #data |
|---------------------------|-------------------|---------|----------------|----------------|-------|
| <i>Single-Document QA</i> | | | | | |
| NarrativeQA | Literature, Film | 18,409 | F1 | English | 200 |
| Qasper | Science | 3,619 | F1 | English | 200 |
| MultiFieldQA-en | Multi-field | 4,559 | F1 | English | 150 |
| <i>Multi-Document QA</i> | | | | | |
| HotpotQA | Wikipedia | 9,151 | F1 | English | 200 |
| 2WikiMultihopQA | Wikipedia | 4,887 | F1 | English | 200 |
| MuSiQue | Wikipedia | 11,214 | F1 | English | 200 |
| <i>Summarization</i> | | | | | |
| GovReport | Government report | 8,734 | Rouge-L | English | 200 |
| QMSum | Meeting | 10,614 | Rouge-L | English | 200 |
| MultiNews | News | 2,113 | Rouge-L | English | 200 |
| <i>Few-shot Learning</i> | | | | | |
| TREC | Web question | 5,177 | Accuracy (CLS) | English | 200 |
| TriviaQA | Wikipedia, Web | 8,209 | F1 | English | 200 |
| SAMSum | Dialogue | 6,258 | Rouge-L | English | 200 |
| <i>Synthetic Task</i> | | | | | |
| PassageCount | Wikipedia | 11,141 | Accuracy (EM) | English | 200 |
| PassageRetrieval-en | Wikipedia | 9,289 | Accuracy (EM) | English | 200 |
| <i>Code Completion</i> | | | | | |
| LCC | Github | 1,235 | Edit Sim | Python/C#/Java | 500 |
| RepoBench-P | Github repository | 4,206 | Edit Sim | Python/Java | 500 |

C.3 Construction of Long CoT Dataset

To simulate Chain-of-Thought (CoT) tasks within long-context, we increased the number of few-shot examples. Specifically, we randomly selected a fixed number of questions and standard CoT answer pairs as prompts, along with the questions to be tested. We chose 25, 47, and 97 few-shot examples, resulting in input lengths of approximately 4K, 8K, and 16K tokens respectively. The few-shot data were sourced from the GSM8K training set. Since the test set does not overlap with the training set, the answers remain undisclosed to the LLM.

C.4 Longbench Results of All Tasks

Due to space constraints, we presented the test results after aggregating task types in Section 5.3. Here, we present the individual results for all tasks. The Table 7 shows that our method surpasses the majority of the SOTAs on most tasks, and the average performance under all budgets and LLMs exceeds all compared methods, demonstrating the effectiveness of our approach.

Table 7: The detailed evaluation results from LongBench of all tasks.

| Budget | Method | Single-DocumentQA | | | Multi-DocumentQA | | | Summary | | | Few-shot Learning | | | Synthetic | | Code | | Average† |
|------------------------------|--------------------|-------------------|--------------|--------------|------------------|--------------|--------------|--------------|--------------|--------------|-------------------|--------------|--------------|--------------|---------------|--------------|--------------|--------------|
| | | NrcvQA | Qasper | MF-en | HopopQA | 2WikiMQA | Musique | GovReport | QMSum | MultiNews | TREC | TriviaQA | SAMSum | PCCount | Pre | LeC | RR-P | |
| Longchat-v1.5-7b-32k | | | | | | | | | | | | | | | | | | |
| Full | Full cache | 20.70 | 29.41 | 43.09 | 33.05 | 24.14 | 14.66 | 30.84 | 22.79 | 26.61 | 66.50 | 83.99 | 40.90 | 0.00 | 30.50 | 52.94 | 56.78 | 36.06 |
| 512 | StreamingLLM | 15.03 | 17.71 | 27.14 | 27.00 | 21.52 | 9.09 | 21.51 | 19.39 | 21.97 | 55.00 | 81.07 | 37.07 | 0.50 | 5.00 | 46.40 | 53.05 | 28.65 |
| | H2O+ | 19.01 | 24.00 | 33.08 | 30.60 | 22.47 | 12.23 | 21.01 | 21.59 | 22.07 | 50.50 | 83.42 | 39.62 | 0.00 | 27.50 | 51.35 | 54.63 | 32.07 |
| | SnapKV | 18.73 | 25.21 | 38.18 | 33.26 | 23.79 | 13.27 | 21.84 | 21.15 | 22.58 | 59.00 | 84.20 | 38.41 | 0.00 | 25.50 | 54.39 | 57.43 | 33.56 |
| | Quest | 16.80 | 31.43 | 38.01 | 27.95 | 23.73 | 10.03 | 27.91 | 22.58 | 25.68 | 60.50 | 81.27 | 39.95 | 0.00 | 41.50 | 51.95 | 50.22 | 34.34 |
| | AttentionPredictor | 17.69 | 28.49 | 41.63 | 34.13 | 23.67 | 14.18 | 28.40 | 21.82 | 25.52 | 64.00 | 84.66 | 40.56 | 1.00 | 25.50 | 54.42 | 55.89 | 35.10 |
| 1024 | StreamingLLM | 16.30 | 20.06 | 32.30 | 28.60 | 21.37 | 9.56 | 25.52 | 20.36 | 23.51 | 60.50 | 82.15 | 39.29 | 1.50 | 6.00 | 52.74 | 53.71 | 30.84 |
| | H2O+ | 18.92 | 24.65 | 37.38 | 32.40 | 22.28 | 12.46 | 22.72 | 21.62 | 24.22 | 59.00 | 84.39 | 39.90 | 0.00 | 28.00 | 53.74 | 55.60 | 33.58 |
| | SnapKV | 19.46 | 26.97 | 38.96 | 34.01 | 23.22 | 14.33 | 23.17 | 21.46 | 24.50 | 64.00 | 84.33 | 39.93 | 0.00 | 28.00 | 53.96 | 57.72 | 34.63 |
| | Quest | 18.51 | 31.09 | 41.32 | 29.92 | 22.95 | 11.35 | 30.16 | 22.67 | 26.52 | 66.00 | 83.35 | 40.86 | 0.00 | 35.00 | 50.77 | 54.16 | 35.29 |
| | AttentionPredictor | 19.36 | 29.50 | 41.67 | 33.64 | 24.30 | 14.91 | 29.92 | 22.30 | 26.09 | 66.00 | 84.85 | 40.58 | 0.00 | 28.00 | 52.22 | 56.54 | 35.62 |
| 2048 | StreamingLLM | 15.52 | 22.66 | 36.20 | 29.03 | 22.15 | 10.13 | 27.59 | 21.04 | 26.20 | 64.00 | 81.93 | 38.62 | 2.00 | 9.50 | 49.78 | 55.46 | 31.99 |
| | H2O+ | 19.10 | 26.62 | 36.82 | 33.23 | 22.66 | 12.83 | 25.13 | 21.93 | 21.09 | 62.50 | 84.65 | 40.60 | 0.00 | 29.00 | 53.33 | 55.99 | 34.09 |
| | SnapKV | 20.02 | 28.69 | 40.61 | 34.13 | 24.02 | 14.67 | 26.05 | 21.82 | 25.59 | 65.00 | 84.71 | 40.89 | 0.00 | 28.50 | 54.93 | 58.44 | 35.50 |
| | Quest | 19.12 | 32.08 | 43.72 | 31.91 | 24.97 | 14.83 | 31.56 | 22.65 | 26.36 | 66.50 | 85.09 | 41.69 | 0.00 | 31.50 | 50.53 | 55.73 | 36.14 |
| | AttentionPredictor | 20.07 | 30.06 | 42.60 | 34.26 | 24.20 | 14.64 | 30.53 | 22.07 | 26.61 | 67.00 | 84.94 | 41.86 | 0.00 | 30.50 | 52.45 | 56.59 | 36.15 |
| 4096 | StreamingLLM | 19.45 | 27.90 | 41.53 | 28.54 | 20.50 | 10.99 | 26.86 | 20.73 | 26.54 | 58.00 | 75.71 | 34.82 | 2.50 | 13.00 | 54.31 | 56.41 | 32.36 |
| | H2O+ | 20.53 | 28.28 | 41.41 | 32.78 | 23.87 | 14.52 | 27.81 | 21.76 | 21.71 | 64.50 | 84.09 | 40.90 | 0.00 | 29.50 | 52.71 | 56.61 | 35.06 |
| | SnapKV | 20.30 | 28.90 | 42.36 | 33.49 | 24.46 | 15.11 | 28.37 | 22.54 | 26.54 | 66.00 | 84.19 | 41.20 | 0.00 | 29.00 | 54.70 | 58.69 | 35.99 |
| | Quest | 19.67 | 29.26 | 43.90 | 32.72 | 23.61 | 12.61 | 31.49 | 22.95 | 26.27 | 67.00 | 84.38 | 41.18 | 0.00 | 31.00 | 51.62 | 55.53 | 35.83 |
| | AttentionPredictor | 20.12 | 29.33 | 42.88 | 34.12 | 24.27 | 15.10 | 30.74 | 22.70 | 26.59 | 67.00 | 84.14 | 41.42 | 0.00 | 29.50 | 53.00 | 56.69 | 36.10 |
| LLaMA-3.1-8B-Instruct | | | | | | | | | | | | | | | | | | |
| Full | Full cache | 29.28 | 45.36 | 56.12 | 56.67 | 48.90 | 32.43 | 33.77 | 25.20 | 27.08 | 74.00 | 91.48 | 40.85 | 5.07 | 99.50 | 56.86 | 48.15 | 48.17 |
| 512 | StreamingLLM | 22.49 | 24.93 | 38.64 | 48.48 | 41.41 | 29.43 | 24.08 | 20.24 | 23.38 | 58.50 | 81.60 | 38.22 | 8.00 | 98.50 | 55.32 | 45.49 | 41.17 |
| | H2O+ | 25.93 | 29.59 | 45.53 | 50.59 | 45.75 | 29.24 | 24.50 | 23.28 | 23.56 | 48.50 | 88.90 | 41.39 | 8.16 | 99.50 | 56.06 | 47.88 | 43.02 |
| | SnapKV | 26.51 | 39.81 | 52.05 | 54.60 | 46.31 | 26.92 | 24.27 | 23.22 | 24.16 | 65.50 | 90.93 | 40.31 | 4.39 | 99.00 | 55.66 | 46.64 | 45.02 |
| | Quest | 25.82 | 44.01 | 53.99 | 58.08 | 43.96 | 28.84 | 32.90 | 24.50 | 26.80 | 70.00 | 88.55 | 39.42 | 11.16 | 99.50 | 51.65 | 42.03 | 46.33 |
| | AttentionPredictor | 27.29 | 45.60 | 57.43 | 56.20 | 48.85 | 32.20 | 30.50 | 24.82 | 26.53 | 68.00 | 91.09 | 40.18 | 13.50 | 99.50 | 56.88 | 45.09 | 47.73 |
| 1024 | StreamingLLM | 24.69 | 27.84 | 42.65 | 48.20 | 37.82 | 26.50 | 26.80 | 21.55 | 22.40 | 64.00 | 89.42 | 40.65 | 8.00 | 94.50 | 56.18 | 46.33 | 42.35 |
| | H2O+ | 26.24 | 36.30 | 48.47 | 53.97 | 45.78 | 27.08 | 26.11 | 23.59 | 25.05 | 53.00 | 88.54 | 40.88 | 9.05 | 99.50 | 55.20 | 49.22 | 44.25 |
| | SnapKV | 27.63 | 41.86 | 52.37 | 55.83 | 46.39 | 27.69 | 26.39 | 24.06 | 25.49 | 70.00 | 90.66 | 40.76 | 8.12 | 99.50 | 55.55 | 49.58 | 46.37 |
| | Quest | 27.46 | 43.58 | 54.95 | 57.22 | 44.53 | 29.86 | 33.64 | 25.37 | 26.68 | 72.00 | 88.61 | 40.05 | 9.55 | 99.50 | 53.92 | 43.82 | 46.92 |
| | AttentionPredictor | 28.50 | 47.35 | 54.99 | 57.53 | 45.91 | 31.63 | 32.52 | 24.51 | 26.78 | 73.00 | 89.54 | 42.12 | 6.49 | 99.50 | 56.96 | 47.43 | 47.80 |
| 2048 | StreamingLLM | 25.79 | 32.35 | 45.03 | 49.84 | 36.71 | 23.29 | 29.31 | 22.43 | 26.83 | 69.00 | 86.87 | 38.53 | 7.25 | 83.00 | 43.32 | 46.66 | 41.64 |
| | H2O+ | 28.07 | 40.35 | 53.22 | 54.81 | 44.75 | 31.77 | 28.20 | 23.50 | 26.37 | 64.50 | 90.71 | 41.32 | 6.71 | 100.00 | 57.97 | 49.19 | 46.34 |
| | SnapKV | 28.00 | 45.34 | 54.98 | 57.97 | 45.89 | 30.50 | 28.92 | 24.29 | 26.32 | 71.50 | 89.36 | 40.71 | 6.64 | 100.00 | 58.79 | 49.90 | 47.44 |
| | Quest | 29.25 | 46.05 | 55.90 | 57.91 | 45.51 | 30.82 | 34.05 | 24.89 | 26.93 | 74.00 | 92.41 | 41.77 | 8.50 | 100.00 | 54.29 | 45.72 | 48.00 |
| | AttentionPredictor | 27.32 | 45.23 | 55.78 | 56.32 | 46.96 | 32.47 | 33.21 | 25.13 | 27.04 | 71.00 | 91.25 | 42.52 | 11.25 | 99.50 | 56.87 | 46.74 | 48.04 |
| 4096 | StreamingLLM | 25.88 | 43.45 | 55.55 | 49.90 | 37.78 | 28.79 | 28.13 | 22.18 | 26.70 | 62.00 | 78.53 | 36.32 | 8.29 | 74.00 | 58.63 | 45.91 | 42.63 |
| | H2O+ | 28.37 | 45.33 | 55.72 | 56.27 | 47.74 | 31.63 | 30.91 | 24.15 | 26.89 | 65.50 | 90.96 | 41.97 | 7.08 | 99.50 | 57.52 | 49.70 | 47.45 |
| | SnapKV | 29.17 | 44.03 | 55.40 | 56.14 | 49.01 | 30.86 | 31.36 | 24.73 | 26.85 | 72.00 | 90.31 | 40.58 | 8.68 | 99.50 | 57.75 | 49.03 | 47.84 |
| | Quest | 29.30 | 46.43 | 54.66 | 55.88 | 47.01 | 30.65 | 34.54 | 25.23 | 26.31 | 71.00 | 89.76 | 43.92 | 6.42 | 100.00 | 55.25 | 45.06 | 47.59 |
| | AttentionPredictor | 28.13 | 45.48 | 55.81 | 56.48 | 49.41 | 30.46 | 33.57 | 24.77 | 27.10 | 72.50 | 90.26 | 41.45 | 9.32 | 99.50 | 55.88 | 46.53 | 47.92 |

C.5 Ablation Study Results

Hyperparameter results. We evaluate the impact of hyperparameters on our method. Specifically, we train the predictor using the default parameters of the main experiment, i.e., $b = 16$, $H = 64$. We employ full attention without sparse computation during training, which is equivalent to performing distribution error calibration at each step, i.e., $M = 1$. Subsequently, we test the performance under different hyperparameters using the trained model. Other parameters during testing remain consistent with the main experiment, with a KV budget of 1K. We evaluate six representative tasks in Longbench. The results are shown in Table 8.

When the block size is 8, we achieve comparable performance to the non-compressed model, demonstrating the effectiveness of our method. Additionally, we significantly mitigate the accuracy drop caused by the increase in retrieval granularity. When $b = 64$, AttentionPredictor outperforms Quest by 10%. For the summary long output task, increasing the frequency of error calibration effectively improves model performance, underscoring the effectiveness of our error calibration method.

Table 8: Results of AttentionPredictor with different hyperparameters.

| LongBench+Longchat | | | | | | | |
|-------------------------|------------|----------|---------|----------|-----------|-------|--------------|
| Hyperparameter | SQA | MQA | Summary | Few-shot | Synthetic | Code | Average |
| | MF-en | HotpotQA | QMSum | TriviaQA | Pre | Lcc | |
| Full Cache | 43.09 | 33.05 | 22.79 | 83.99 | 30.50 | 52.94 | 44.39 |
| History Step | 16 | 41.83 | 34.00 | 22.22 | 84.45 | 28.00 | 51.87 |
| | 32 | 41.60 | 33.90 | 22.32 | 84.81 | 30.00 | 52.53 |
| | 64 | 41.67 | 33.64 | 22.30 | 84.85 | 28.00 | 52.22 |
| | 128 | 41.51 | 34.39 | 22.45 | 84.35 | 26.00 | 52.96 |
| Calibration Step | 1 | 42.89 | 33.27 | 22.35 | 84.70 | 28.50 | 52.53 |
| | 2 | 42.47 | 33.61 | 22.43 | 84.90 | 28.00 | 52.13 |
| | 5 | 41.67 | 33.64 | 22.30 | 84.85 | 28.00 | 52.22 |
| | 10 | 41.10 | 33.87 | 22.37 | 84.85 | 28.00 | 52.36 |
| | 20 | 41.54 | 33.99 | 22.12 | 84.90 | 28.00 | 52.50 |
| Block Size | 8 | 43.09 | 34.61 | 22.38 | 85.29 | 28.00 | 52.76 |
| | 16 | 41.67 | 33.64 | 22.30 | 84.85 | 28.00 | 52.22 |
| | 32 | 40.85 | 34.47 | 22.46 | 84.87 | 25.00 | 53.02 |
| | 64 | 42.60 | 34.04 | 22.01 | 84.85 | 19.00 | 52.86 |